Determining external loads of trees by analysing the stem geometry

G. Benderoth, G. Silber

FH Frankfurt, University of Applied Sciences, Institute for Material Science, Nibelungenplatz 1, D-60318 Frankfurt, Germany

Abstract

According to the more abundant storm events in the last decade of the 20th century the damages in forests are rising (PETERSON, 2000). For an adequate forest policy it would be helpfully to know how trees will estimate their wind load risk. This paper presents a simple model based on the hypothesis of *Constant Stress* relating the stem geometry with the forces a stem has to resist like crown, wind and body load. To validate this model the stem geometry and the crown weight of juvenile Italian oak plans (Quercus ilex) have been measured. The result of the comparison between the measurements and the model predictions suggests that the hypothesis of *Constant Stress* is used by trees as a building rule for their stems.

Key words: optimal stem growth strategies, constant stress hypothesis, wind load bearing capacity

Introduction

There are two basic mechanical features a tree stem has to fulfil. It has to guarantee the conduction of water and minerals from the root to the leaves and a flow of organic material in the opposite direction and it has to keep the crown upright. This means that the stem neither buckles under normal forces like crown and its own body load, nor breaks under wind, water and ice load. Plants with secondary growth run a material strategy (BENDEROTH et al., 2000) that means they fix their material properties quite early in their life but show a variable growth of their stem geometry. Having a fixed material property the buckling limit only depends on the stem geometry and the crown load. The

Email addresses: benderot@fb2.fh-frankfurt.de (G. Benderoth), silber@fb2.fh-frankfurt.de (G. Silber).

stem geometry can be varied according to the crown load development. For huge crowns a small stem with big diameters and for small crowns a slender stem with small diameters is built by the organism. To achieve an adequate stem growth the plant must have a construction rule, which makes such a growth possible. An appropriate growth rule is the law of *Constant Stress* recently reintroduced by MATTHECK (1990). The intention of this article is to verify this hypothesis by a model and an adequate experiment.

Model

Stem growth like almost all other features of organisms is subject of an optimisation process. Thus growth should take place at maximum mechanical safety with a minimum amount of material at its least possible material quality. One necessary condition to obtain this goal is, to avoid notch stresses. Because of the particular load case of stems the highest stress will occur at the surface of the construction (see fig 2). Therefore a geometry generating a homogenous stress distribution at the stem's surface fulfils this requirement (MATTHECK, 1990) (MATTHECK, 1992) because such a construction avoids notch stresses.

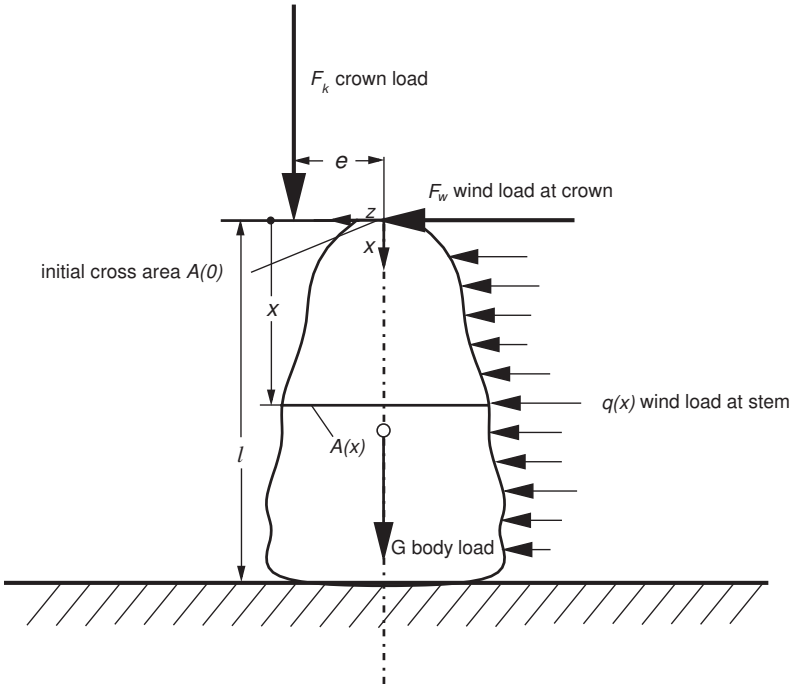

Fig. 1. Sketch of the load conditions of a plant stem

In fig. 1 all sources of stress at a circular upright standing lever are shown. The stress of such a structure at an arbitrary chosen cross section $A(x)$ is given by:

$$\sigma(x,z) = \frac{N(x)}{A(x)} + \frac{M(x)}{I(x)}\, z(x) \tag{1}$$

with $N(x)$ are forces in longitudinal direction, $M(x)$ are moments perpendicular to the longitudinal direction, $A(x)$ the cross section area of the beam, $I(x)$ the moment of inertia and z a cross section coordinate.

Assuming the *Constant Stress* hypothesis for the outer fibre of the lever in the compression case and furthermore assuming for the longitudinal forces:

$$N(x) = F_k + \gamma \int_{\xi=0}^{x} A(\xi)\, d\xi$$

for the moments:

$$M(x) = F_w\, x + F_k\, e + \int_{\xi=0}^{x} q(\xi)\, (x-\xi)\, d\xi$$

and a circular cross section, the following model is derived from equation (1) (for calculation details see Appendix A):

$$\left[d(x)^3 + S + K\, x + L\, \frac{x^2}{2}\right] d'(x) - d(x)\, \left[B\, d(x)^3 + K + L\, x\right] = 0 \tag{2}$$

by using the definitions:

$$B := \frac{\gamma}{2\,\sigma_0}, \qquad K := \frac{16\, F_w}{\pi\, \sigma_0}, \qquad L := \frac{16\, q_0}{\pi\, \sigma_0}, \qquad S := \frac{16\, F_k\, e}{\pi\, \sigma_0} \tag{3}$$

Equation (2) can be solved numerically with the initial condition $d(0) = d_0$. An analytic solution can only be obtained for particular solutions. Of special interest are the particular solutions concerning the wind load. This load is divided into two parts, one acting upon the stem (q_0) and the other upon the crown (F_w). For the particular case $q_0 = 0$ eq. (2) can be solved (for calculation see AppendixA). The solution is:

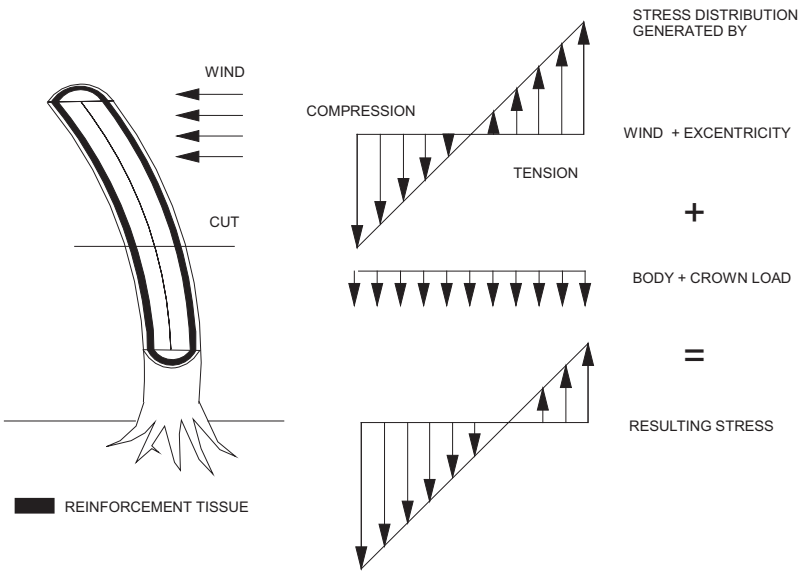

Fig. 2. Stress distribution at a cross section of a stem caused by external loads

$$0 = \frac{S\,[B\,d_0^3 + K]^{\frac{1}{3}}}{K\,d_0} - \frac{S\,[B\,d(x)^3 + K]^{\frac{1}{3}}}{K\,d(x)} - \frac{S\,[B\,d(x)^3 + K]^{\frac{1}{3}}\,x}{d(x)} + \int_{d_0}^{d(x)} \frac{\zeta}{(B\,\zeta + K)^{\frac{2}{3}}\,d\zeta} \tag{4}$$

The solution of the last term in eq. (4) is a hyper geometric series. Because of this an explicit representation of eq. (4) can't be given, but the envelopes of eq. (4) can be derived. One envelope can be obtained, if F_w vanishes. For this case the solution of eq. (4) is (for calculation see Appendix A):

$$0 = \frac{S\,[d(x)^3 - d_0^3]}{3\,d(x)^3\,d_0^3} - B\,x + ln\frac{d(x)}{d_0} \tag{5}$$

The opposite envelope can be generated from eq. (4) for the case that the wind load is much larger than the body weight represented by $\gamma = 0$. For this case the solution is:

$$0 = d(x)^3 + \frac{2\,S - d_0^3}{d_0}\,d(x) - 2\,(S + K\,x) \tag{6}$$

The second particular solution is gained when $F_w = 0$ is set. In this case eq. (2) becomes:

$$0 = \left[d(x)^3 + S + L\,\frac{x^2}{2}\right]\,d'(x) - d(x)\,\left[B\,d(x)^3 + L\,x\right] \tag{7}$$

The envelopes of eq. (7) can also be generated ($q_0 = 0$ or $\gamma = 0$). The solution of (7) for $q_0 = 0$ is identical with eq. (5). For $\gamma = 0$ the solution is (see Appendix A):

$$0 = d(x)^3 + \frac{S - d_0^3}{d_0}\,d(x) - \left(S + \frac{L\,x^2}{2}\right) \tag{8}$$

The envelopes (6) and (8) differ only quantitatively but not qualitatively. That means the wind load on the stem has the same effect as the wind load on the crown in this model. Or in other words, any superposition of q_0 and F_w has the same effect as q_0 or F_w alone. Therefore the sub model (4) is as meaningful as the model itself.

A further simplification of the model can be made. All test specimens used for this investigation show no eccentricity ($e = 0$) of the crown, thus eq. (4) reduces to:

$$0 = -\frac{[B\,d(x)^3 + K]^{\frac{1}{3}}\;x}{d(x)} + \int_{d_0}^{d(x)} \frac{\zeta}{[B\,\zeta^3 + K]^{\frac{2}{3}}}\,d\zeta \tag{9}$$

For the rest of the investigation sub model (9) will be considered.

The envelopes of eq. (9) can be calculated from eq. (5) and eq. (6). The first envelope is:

$$d(x) = d_0\,e^{\frac{\gamma}{2\,\sigma_0}\,x} \tag{10}$$

The second is:

$$0 = d(x)^3 - d_0^2\, d(x) - 2\, K\, x \tag{11}$$

Both envelopes are monotonous and steady. In the case of eq. (10) the function is strictly, progressively rising whereas eq. (11) is strictly digressively rising. In a normalised plot all curves derived from eq. (10) will lay below the 45° line whereas all curves derived from eq. (11) will lay above it. Hence all solutions of eq. (9) will lay between these two solutions.

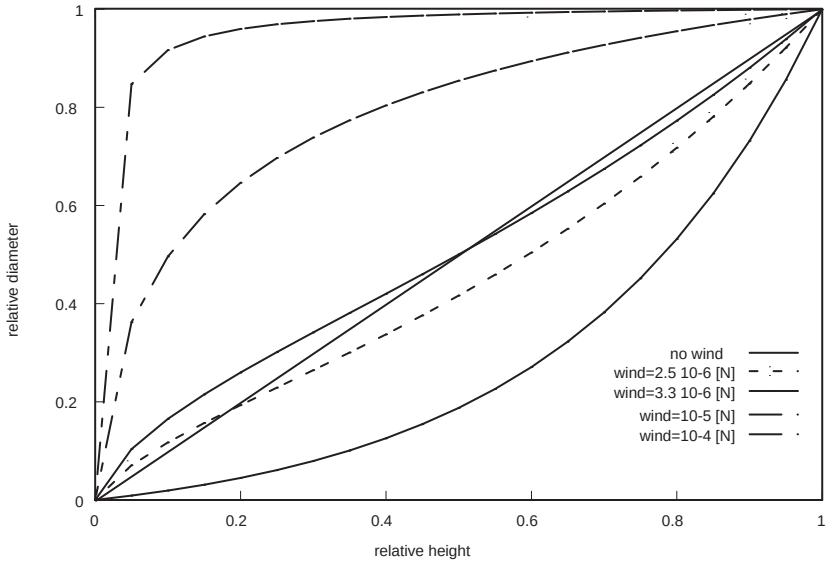

Fig. 3. Normalised plot of the model (eq. (9))

Fig. 3 shows a relative plot of eq. (9). The parameter crown and wind load were chosen arbitrarily.

A stem ignoring wind load will always grow by an exponential curve of its stem shape, whereas the rising influence of the wind changes the shape towards to a barrel shaped contour (see fig. 3).

The Test

To verify the model, the geometry of the stem and the forces acting on the stem have to be measured.

The test specimens were freshly cut, three years old juvenile oak shoots (Quercus ilex) from the Tuscany in Italy. The specimens came from two different sites. The specimen of the first sample (CI) grew up at a site with ambient atmospheric CO_2 concentration, whereas the second sample (EI) came from a dip with elevated CO_2 conditions caused by volcanic activities. The specimens of this sample show a much enhance growth compared to the specimens of the first sample.

From all test specimens the total height was taken from the top spot, where all remaining branches were cut and taken as crown weight, down to the spot where the stems were cut. To obtain geometric data of the test specimens to evaluate the model it is necessary to distinguish between local and global growth effects induced by stress. Each branch inserting at the stem transmits a mechanical moment, which will cause growth at the stems surface to equalise the stress at this insertion spot. This local stress effects the stem's shape below and above each particular insertion spot (node). To avoid these local effects the nodes where the branches insert at the stem were not taken as measuring sites. Instead of these sites the diameters in the middle of two nodes were measured. The distance from these points to the top of the stem was taken as the height of that diameter. After measuring the diameter to height relation each branch on the stem was cut and the weight of it including all twigs and leaves was measured by a digital balance (SATORIUS). The distance of the middle of the cutting area to the top of the stem was taken as the inserting height of the branch at the stem. Diameters were measured by a digital calliper and the lengths by a meter stick.

To determine the stem's density pieces from the base of each stem were taken as long as the stems were humid. All densities were only slightly different from the density of water (0.98-1 kg/dm^3). The density was determined by the method of ARCHIMEDES on the same digital balance used for determining the weights of the branches.

Results and Discussion

There is a huge difference in the quality of the different loads acting upon the stem. The loads (crown and body load) generated by the plant itself, are and will exist through the life time of the plant and can also be measured over this period. This kind of loads can be characterised as internal or permanent loads. Whereas loads not generated by the system itself (e.g. wind, water and ice load) are neither permanent nor are their magnitudes fixed. These loads are external or temporary loads. Since their appearance and their magnitude are not certain, their impacts on the plant have to be estimated by the plant

Table 1
Example of a data set (CI 10)

Diameter [mm]	Height [mm]	Mass [g]	Height [mm]
5.9	50	19,4	0
6.2	90	2.3	20
6.3	125	3.3	30
6.5	175	2.4	50
7.0	235	3.3	80
7.0	350	0.4	150
7.0	390	0.7	200
7.6	430	1.3	250
7.7	500	0.9	350
8.2	600	0.6	500
8.7	700	1.0	600
9.1	800	0.7	700

itself.

Most of these loads are parameters in the model. How can these parameter determined by experiments ? The permanent load body load depends on the density of the material. This density is measurable by the plant and by the experiment, too. Unfortunately the density depends on the hydration level of the stem. Thus you will only get a temporary image of the actual density value by the experiment. Even for the plant a maximum estimate will be the appropriate value. The worst case approximation is the density of water. This value is used within the evaluation of the model.

Because of the growth type of plants, crowns can only grow and can hardly loose weight by themselves. Only by external events such as breaks of branches a loss of weight can be attained. So if no breakage are detectable, the weight of the crown is the worst case estimation for the crown load at the moment the experiment is carried out. Thus the measured crown load is the right estimation for the parameter crown load and can be used as a control value for the goodness of the model.

Eccentricity is also an internal parameter. It can be detected by measuring the contour of the plant. Difficulties arise in determining the centre of weight of the crown to have an exact estimate for this parameter. In the case of the test specimens used for this study the eccentricity is ignored, since all specimens were almost completely grown upright.

The parameter for the temporary loads can't be measured. Measurable is the response of the stem of each test specimen to the wind load. But this response does not reflect a functional relation between the magnitude of the wind load and the stem shape. Due to the temporary character of the load the organism is able to run different strategies, from ignoring to over estimating the load risk.

The analysing procedure is to estimate the parameters F_w, F_k and d_0 from the comparison of the model equations with the data by minimising the distance of a data point to its estimated value by the model (*Least Square Approximation*).

As described in the model section and shown in fig. 3 a normalised diameter to height relation which always lays below the 45 line can be mapped by sub model (10). Thus analysis started with a normalise plot of the data (see fig. 4 and 5) to decide which stems can be mapped with which sub model. This was done for all stems.

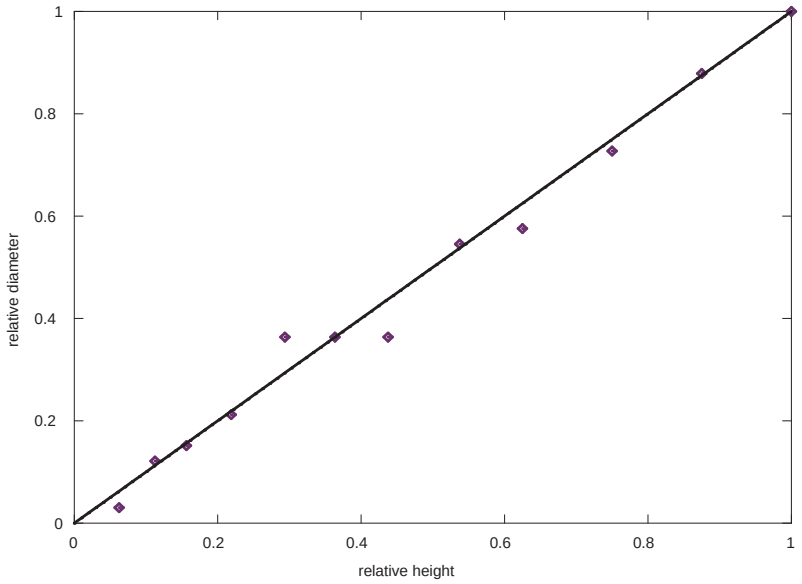

Fig. 4. A normalised plot of the geometric data of stem CI-10

Regardless of the normalised plot analysis the parameter fit was carried out with both sub models for all test specimens. In the case of sub model (10) the measurable parameters crown load F_k can be derived from the initial stress σ_0 by the relation:

$$\sigma_0 = \frac{4\,F_k}{\pi\,d_0^2} \tag{12}$$

Inserting relation (12) into eq. (10) and applying the natural logarithm to it the model equation (10) transforms into:

$$\ln[d(x)] = \ln[d_0] + \frac{\gamma\,\pi\,d_0^2\,x}{8\,F_k} \tag{13}$$

The estimation for F_k and d_0 was made by a *Least Square Fit*:

$$\Theta = \sum_{i=1}^{n} \left\{ \ln[d_0] + \frac{\gamma\,\pi\,d_0^2\,x_i}{8\,F_k} - \ln[d(x_i)] \right\}^2 \stackrel{!}{=} \min \tag{14}$$

Calculation details are given in Appendix B. The equation for determining the crown load and the initial diameter are:

$$\begin{aligned} \ln[d_0] &= \frac{\sum \ln d_i \;\sum x_i^2 - \sum x_i \;\sum x_i \;\ln d_i}{n\;\sum x_i^2 - (\sum x_i)^2} \\ F_k &= \frac{\gamma\,\pi\,d_0^2\;\sum x_i^2}{8\,(\ln d_i\;\sum x_i - \ln d_0\;\sum x_i)} \end{aligned} \tag{15}$$

where x_i and d_i are the experimental data and n is the number of data points.

Using sub model (9) for the analysis a linear approach for the optimisation procedure can not be used. To solve this optimisation problem, a simple stochastic procedure (*Monte Carlo*) was used. For the sake of comparability the assumption was made that σ_0 of model (10) is equal to σ_0 of model (9). In this case relation (12) is also valid for sub model (9) and can be used for the calculation of F_k. Thus estimates for the intervals of the parameter for the *Monte Carlo Algorithm* could be centred around the results of the linear fit for d_0 and F_k. For F_w a large interval ranging from 0 to 10 N was chosen. The termination criteria for the *Monte Carlo* routine was to obtain almost the same or even a better *Sum of Least Squares* as for the linear optimisation.

Results of the parameter fit are given in table 2 and 3. Where F_k emp. is the measured crown load, F_k lin. and F_k non are the estimated crown loads of the different sub models (10, 9), err lin and err non lin the *Sum of Least Square* for the different models and F_w the estimated wind load from the model.

The termination criteria for the *Least Square* optimisation was accomplished in almost all cases.

Table 2
Results of the test specimens of series CI

	F_k *emp.*	F_k *lin.*	*err. lin.*	F_k *non*	*err. non lin.*	F_w
CI 1	1.11E-01	3.23E-01	4.43E-07	5.40E-06	1.70E-06	8.62E-04
CI 2	8.18E-02	6.81E-02	1.68E-05	9.16E-02	6.38E-05	1.21E-03
CI 3	3.63E-01	2.19E-01	1.25E-06	4.72E-01	3.67E-06	1.20E-03
CI 4∗	2.13E-01	1.24E-01	1.89E-06	2.26E-01	1.02E-06	5.66E-04
CI 5∗	1.56E-01	2.35E-01	7.58E-06	1.65E-01	4.09E-06	9.74E-04
CI 6	2.92E-01	4.08E-01	3.16E-06	3.68E-01	3.79E-06	9.27E-05
CI 7	1.61E-01	1.05E-01	7.12E-07	1.35E-01	1.74E-06	5.67E-04
CI 8∗	4.49E-02	1.10E-01	1.06E-05	6.66E-02	8.53E-06	9.27E-04
CI 9	1.88E-01	1.97E-01	1.58-06	2.26E-01	5.41E-06	1.03E-03
CI10	2.50E-01	2.43E-01	1.64E-07	5.92E-01	4.11E-07	1.08E-03
CI11	3.85E-01	2.93E-01	8.18E-07	3.82E-01	7.44E-05	1.46E-03
CI12	2.38E-02	4.26E-02	1.20E-06	8.48E-02	9.98E-06	5.08E-04
CI13	5.50E-01	1.31E-01	1.74E-06	1.82E-01	2.21E-06	7.66E-04
CI14	5.85E-01	3.81E-01	8.63E-06	5.52E-01	1.05E-05	1.86E-03

∗ optimal with wind load

The predicted crown load is for both sub models of the same magnitude as the empirical value. Because eq. (10) is a sub model of (9), one may expect, that in all cases the *Sum of Least Squares* in the non linear case must be equal or smaller than those of the sub model (10). Due to the large variation in the test data this is not always the case.

Because of this large variation and of the nature of the parameter F_w the qualitative behaviour of the model can be evaluated. Exploiting another feature of the model makes it possible to evaluate the capacity of the model for predicting the wind bearing capacity of an individual plant. As pointed out in the model section sub model (10) is a strictly, monotonously and progressively rising function. In a normalised plot such a function will always stay below the bisection whereas sub model (9) will always show that at least a part of it is above the 45 line. So by inspecting the normalised plots of the test data a separation between those stems including wind load and those which do not is possible (see fig. 4). Because of the errors the data are affiliated with the plots were characterised with sub model (10) when 3/4 of the data points lay below the bisection. All the other data sets were assigned to sub model (9). Asterisks in tab. 2 and 3 indicate the test specimens belonging to sub model (9).

Table 3
Results of the test specimens of series EI

	F_k *emp.*	F_k *lin.*	*err. lin.*	F_k *non*	*err. non lin.*	F_w
EI 1∗	1.18E-01	5.49E-02	1.31E-05	6.94E-02	4.03E-06	5.66E-04
EI 2	5.66E-02	8.38E-02	2.02E-05	8.48E-02	1.60E-05	5.08E-04
EI 3∗	3.82E-02	6.19E-02	8.30E-06	7.58E-02	6.67E-06	2.00E-04
EI 4	2.51E-02	2.46E-02	7.44E-06	5.85E-02	1.10E-05	8.34E-04
EI 5	4.26E-01	2.57E-01	2.14E-06	6.49E-01	3.05E-06	9.18E-04
EI 6∗	4.03E-02	4.02E-02	2.02E-05	6.17E-02	6.73E-06	1.37E-03
EI 7	1.90E-02	3.02E-02	2.19E-05	8.07E-02	8.67E-05	9.18E-04
EI 8∗	1.55E-01	8.33E-02	8.31E-06	8.48E-02	7.13E-06	5.07E-04
EI 9∗	3.41E-02	8.58E-02	3.46E-05	6.93E-02	1.28E-05	5.67E-04
EI 10∗	1.59E-02	5.67E-02	7.23E-06	6.93E-02	4.23E-06	5.67E-04
EI 11∗	3.39E-02	4.73E-02	1.87E-05	5.74E-02	2.52E-05	7.66E-04
EI 12	3.27E-01	3.09E-01	1.50E-06	2.89E-01	5.93E-06	1.03E-03
EI 14∗	7.05E-02	8.54E-02	2.00E-05	1.82E-01	6.39E-06	1.63E-03

∗ optimal with wind load

As discussed in the model section testing the wind bearing capacity is only possible in an indirect way. The hypothesis is:

If the model is able to predict the wind load bearing capacity, the prediction of the crown load will be more precise if the right sub model according to the normalise plot segregation is used. For testing this hypothesis a *Goodness of Fit* test was made with:

$$\chi^2_{emp} = \sum_{i=1}^{n} \frac{\left(F_{k_i}^{data} - F_{k_i}^{model}\right)^2}{F_{k_i}^{model}} \tag{16}$$

with n the number of test specimens

For a significance level of 1% and n-1 degrees of freedom. Results are given in tab.4 and 5.

For series CI the hypothesis holds. If one tries to predict the crown load with the wrong sub model the prediction fails. In the case of EI the result is ambiguous. Only a trend towards the result of the *Goodness of Fit* test in the series of EI can be recognised. This fact is probably due to the fertilisation

Table 4
Goodness of fit test for the CI series of test plants with an error of 1%

	emp vs. lin	*emp vs. non lin*	*DOF*	χ^2 *at* $\alpha = 0.01$
linear	0.9810	2.5790	10	2.5880
non linear	0.1730	0.0119	2	0.0200

Table 5
Goodness of fit test for the EI series of test plants with an error of 1 %

	emp vs. lin	*emp vs. non lin*	*DOF*	χ^2 *at* $\alpha = 0.01$
linear	0.0879	0.3808	4	0.3000
non linear	0.2725	0.5078	7	1.2400

effect of the enhanced atmospheric CO_2 content the sample was exposed to. This enhanced CO_2 content causes an increased growth of the plants of this sample compared to the CI ones. Thus, the distances between two nodes are much smaller in the EI than in the CI sample. This generates a much greater overlay of local and global growth induced by the loads of the local branches and the rest of the plant. This effect can be detected by the sums of the least squares for both sample. The magnitude of these sums are approximately one decimal power larger in the EI sample compared to the CI one (see tab. 2 and 3).

Testing the empirical crown loads vs. the model results for the linear and the

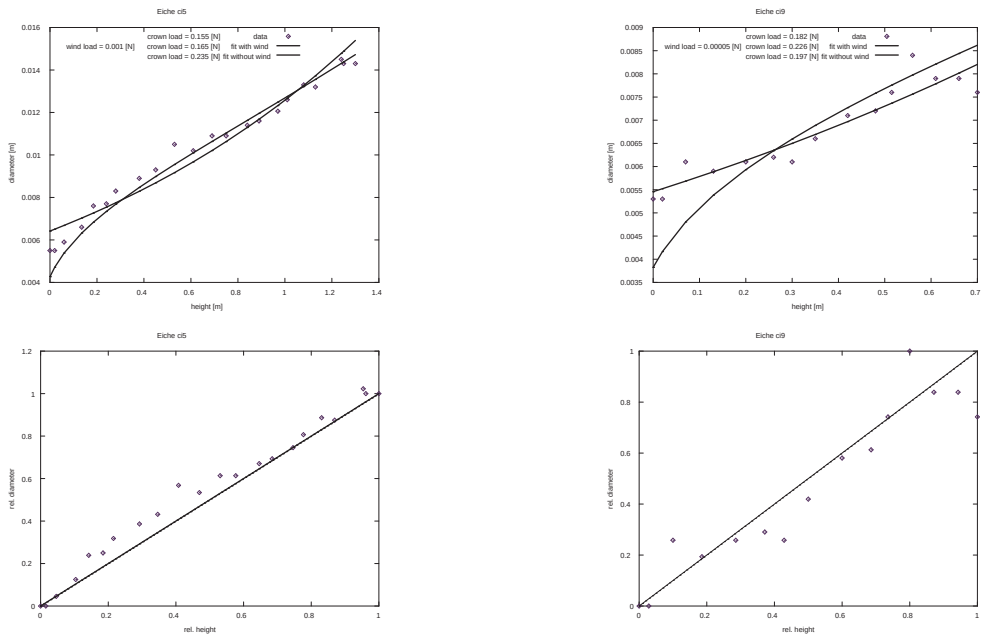

Fig. 5. Examples of relative data and fit plots for different test specimens. The plots on the left side show a case for which the model including wind load suited better. The plots on the right side show the case for the model without wind load.

non linear case shows an average deviation of the crown loads of 25% for model (10) and of 15% for model (9). A test of the deviation of the mean values of the crown loads show no significant at a significance level of 1% in both cases (see tab. 6):

Table 6
Testing the deviations of the predicted crown loads from the test data for Series CI

	mean emp	*mean model*	*calc. t-value*	*distr. t-value*
model (10)	0.2480	0.185	0.89	2.58
model (9)	0.13	0.15	0.25	4.5

Because copies of such an age do not show an explicit crown, the test data of the crown load were modified. For each measured diameter the hole load caused by inserting branches and the parts of the stem (approximated by a truncated cone) above this locus were added (see tab. 1). The *Least Square* estimation was done for all different stem sections down to five geometric data points of the stem's diameter. Three different data sets from the CI series with a smooth function pattern were chosen, to minimise the overlay between local and global impacts of the stresses of the external forces.

Table 7 shows the results for a test specimen suited for sub model (9) and sub model (10). Even under this difficult condition the model is able to predict the loads in an acceptable range with the qualitative correct model version.

Finally the parameter σ_0 has to be discussed. In addition to the buckling boundary there is another boundary for the growth of tree stems. Each material is only able to resist a certain maximum compression stress applied to it. If this stress limit is exceeded the material starts to disaggregate. This stress σ_l also exists for wood. According to the hypothesis of *Constant Stress* the compression stress at any place of the stem is equal to the stress at the crown insertion site. Thus the following relation holds:

Table 7
Results of two example test specimens at different heights and crown loads

	F_k *emp.*	F_k *lin.*	*err. lin.*	F_k *non*	*err. non lin.*
CI 4∗	2.13E-01	1.24E-01	1.89E-04	2.51E-01	1.02E-04
CI 4.1∗	2.87E-01	1.51E-01	1.56E-04	4.10E-01	4.07E-05
CI 4.2∗	5.99E-01	2.18E-01	8.07E-05	3.62E-01	6.19E-05
CI 4.3	6.28E-01	3.45E-01	1.05E-05	3.81E-01	1.08E-05
CI 4.4∗	6.58E-01	3.64E-01	1.30E-05	5.34E-01	9.36E-06
CI 4.5∗	6.54E-01	3.80E-01	9.91E-06	7.72E-01	7.33E-06

$$\sigma_l > \sigma_0 = \frac{4\,F_k}{\pi\,d_0^2} \tag{17}$$

Because of this fact it would be reasonable to run a strategy $\sigma_0 = const$ more or less close to σ_l. Due to this reasoning a linear correlation must be detectable between the square of the stem's diameter at the crown insertion site and the crown load.

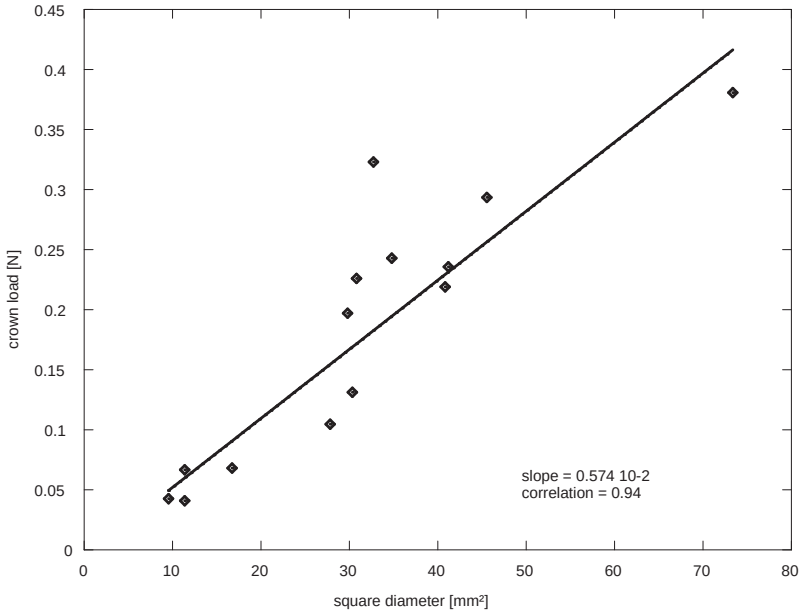

Fig. 6. Linear regression plot of the square of d_0 and the crown load F_k for the CI data set

The regression plot in fig. 6 indicated that this seems to be the strategy of the plants. Particularly because the regression analyses shows a correlation coefficient close to one (0.94).

Conclusion

The model shows a good accordance between the predicted and the measured crown load (see tab. 6). Furthermore it could be shown that correct predictions of the crown load are strongly related with usage of the right sub model (see tab. 4 and 5). That means the parameter wind load is needed for a correct prediction, hence that figure can be taken as the reaction of the plant to resist wind loading. Because storm events are random events concerning their

occurrence and their magnitude calculating the effect of the wind impact on the tree, which is highly non linear procedure (SILAS, 2002), will not solve the problem at all. The random character of storm event forces trees to run a particular strategy for resisting storm impacts. Besides the random character of the storm impacts an investment into wind resistance lowers the possible height of the stem. This fact can negatively effect the production capability of the plant. For that the wind resistance strategy of the plant may be quite different, if it lives under heavy light competition, compared to one with low light competition. The magnitude of the wind force does not reflect a direct correlation between the wind speed and its impact on the tree. But it tells us the relative strategy relation of the different trees among each other. This argument is also supported by the statement of WOOD (1995) that trees own mechanisms to damp heavy swaying under wind load so that the major reason for breaking and uprooting of the plants is the load itself.

In this study the model was applied to juvenile plants. The model itself doesn't own any restrictions concerning the plant species, beside they must show secondary growth, or its age. Therefore it should also work for other plants than oaks and for adult plants, particularly because adult plants exhibit a much more distinguishable stem and crown compared to juvenile ones. Thus adult plants should show even much better results.

Furthermore a proportional relations between stem mass and root radius is reported (MATTHECK et al., 1995). That means, that the different parts of the tree are in sound relation to each other to avoid weak points of the construction. These facts indicate that the calculated wind load capacity is not only a measure for the stem but for the whole plant.

Finally the segregation of the test specimens between ambient and enhanced CO_2 conditions point out differences in in the growth strategies of the plants. The only obvious difference was that the enhance growth of the CO_2 treated specimens caused problems in applying the model. The difference number of specimens showing a wind load resistance (twice as much as in the ambient CO_2 case) can also be due to a higher variability of juvenile growth pattern or to a different wind regime at the two sampling sites.

Acknowledgement

The authors want to thank Antonio Raschi from the CNR for Agrometeorology in Florence, Italy for providing us with the test specimens.

A Appendix Calculation

Equation (1) gives a general description of the stress distribution of a beam at an arbritrary cross section $A(x)$ in the plane for any longitudinal load and transversal moments.

For an optimal shape stem the hypothesis of *constant stress* is applied to (1) meaning that the stress at the outer fibre of the beam has to be constant. Or in other words $\sigma(x, z = \mp z_o(x)) = \sigma_{0\,C}^{T} = const.$ With this condition equation (1) becomes:

$$\sigma_{0\,C}^{T} = \frac{N(x)}{A(x)} \mp \frac{M(x)}{I(x)}\, z_0[x] \qquad \forall\, x\, \epsilon\, [0,\ l] \tag{A.1}$$

The $\mp$ sign in (A.1) indicates that there are different *constant stresses* at the outer fibre due to the loading scenario (tension or compression see fig. 2). But these fibres can be set individually constant.

An optimal stem shape means one has to consider $A(x)$ in equation (A.1). For analysing $A(x)$ one has to differentiate (A.1) with respect to x because $A(x)$ is the integration limit of the moment of inertia ($I(x) = \int_{A(x)} z^2\, dA$) in(A.1). Thus equation (A.1) becomes:

$$0 = \frac{N(x)}{A(x)} \left[\frac{N'(x)}{N(x)} - \frac{A'(x)}{A(x)}\right] \mp M(x) \frac{z_o(x)}{I(x)} \left[\frac{z_o'(x)}{z_o(x)} - \frac{I'(x)}{I(x)} + \frac{M'(x)}{M(x)}\right] \tag{A.2}$$

Resolving equation (A.1) for $N(x)$ and insert this expression into (A.2), one finally gets for the general description of an optimised tension / compression loaded beam:

$$0 = \left[\frac{N'(x)}{A'(x)} - \sigma_{0\,C}^{T}\right] \mp M(x) \frac{z_o(x)}{I(x)} \frac{A(x)}{A'(x)} \left[\frac{z_o'(x)}{z_o(x)} + \frac{A'(x)}{A(x)} - \frac{I'(x)}{I(x)} + \frac{M'(x)}{M(x)}\right] \tag{A.3}$$

For the particular scenario given in fig. (1) some specifications have to be made. First only the compression part will be taken into consideration (for calculation convenience the + was taken). Thus $\sigma_0^{T} = \sigma_0$. Second for the cross

section a circular one is assumed. Thus one gets for the cross area, the cross section variable and for the moment of inertia:

$$A(x) = \frac{\pi}{4} d(x)^2,\ z_0(x) = \frac{d(x)}{2} \text{ and } I(x) = \frac{\pi}{64} d(x)^4$$

Using all these relation for eq. (A.3) one gets:

$$0 = [2\, N'(x) - \sigma_0\, \pi\, d(x)\, d'(x)] + 16[d(x)\, M'(x) - d'(x)\, M(x)] \tag{A.4}$$

According to fig. (A.1) for the longitudinal forces $N(x)$ holds:

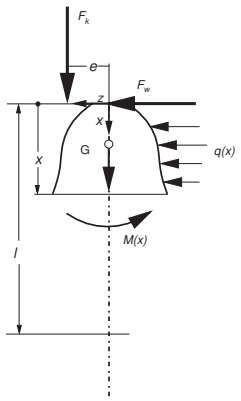

Fig. A.1. *Cut face of the loads for the model*

$$\begin{aligned} N(x) &= F_k + \gamma \int_{\xi=0}^{x} A(\xi)\, d\xi = F_k + \frac{\gamma\, \pi}{4} \int_{\xi=0}^{x} d(\xi)^2\, d\xi \\ N'(x) &= \frac{\gamma\, \pi}{4}\, d(x)^2 \end{aligned} \tag{A.5}$$

and for the moments $M(x)$:

$$M(x) = F_w\, x + F_k\, e + \int_{\xi=0}^{x} q(\xi)\,(x-\xi)\,d\xi = F_w\, x + F_k\, e + q_0\,\frac{x^2}{2} \quad \text{(A.6)}$$
$$M'(x) = F_w + q_0\, x$$

with the simplification $q(\xi) = const = q_0$

Equations (A.5) and (A.6) inserted into equation (A.4) results in:

$$0 = \left[d(x)^3 + S + K\, x + L\,\frac{x^2}{2}\right] d'(x) - \left[B\, d(x)^4 + K\, d(x) + L\, x\, d(x)\right] \quad \text{(A.7)}$$

with the definitions given in (3)

Eq. (A.7) is a first order non linear differential equation of the form $P(x, d(x))dx + Q(x, d(x))dd(x) = 0$. In the case that $\frac{\partial P}{\partial x} = \frac{\partial Q}{\partial d}$ the equation is called an exact differential equation. In the case of (A.7) an exact differential equation doesn't exist because:

$$\begin{aligned} P(x, d(x)) &= -B\, d(x)^4 - K\, d(x) - L\, x\, d(x) \\ Q(x, d(x)) &= d(x)^3 + S + K\, x + L\,\frac{x^2}{2} \\ \frac{\partial P}{\partial d} &= -4\, d(x)^3 - K - L\, x \neq \frac{\partial Q}{\partial x} = K + L\, x \end{aligned} \quad \text{(A.8)}$$

Finding a factor $\mu(x, d(x))$ satisfying this condition eq. (A.7) can be made exact. The following differential equation holds for the integration factor (BRONSTEIN (1980)):

$$\left(\frac{\partial P}{\partial d(x)} - \frac{\partial Q}{\partial x}\right) = Q\frac{\partial \ln \mu}{\partial x} - P\frac{\partial \ln \mu}{\partial d(x)} \quad \text{(A.9)}$$

According to (A.8) the left side of (A.9) is a function of x and $d(x)$. Thus an integrating factor can not be found and a solution of (A.7) can only be given numerically.

Partial solutions of (A.7) can be given. Ignoring q_0 the lhs of (A.9) is only

a function of $d(x)$. Thus μ is also only a function of $d(x)$. So function (A.9) degrades to:

$$\left(\frac{\partial P}{\partial d(x)} - \frac{\partial Q}{\partial x}\right) = -P\frac{\partial \ln \mu}{\partial d(x)} \tag{A.10}$$

Resolve (A.10) for μ:

$$\mu = e^{-\int \frac{1}{P}\left(\frac{\partial P}{\partial d(x)} - \frac{\partial Q}{\partial x}\right) dd(x)} = d(x)^{-2}\left(B\, d(x)^3 + K\right)^{-\frac{2}{3}} \tag{A.11}$$

Multiplying (A.7) by (A.11):

$$0 = Q_1 dd(x) + P_1 dx = \frac{d(x)^3 + S + K\, x}{d(x)^2\left[B\, d(x)^3 + K\right]^{\frac{2}{3}}} dd(x) - \frac{\left[B\, d(x)^3 + K\right]^{\frac{1}{3}}}{d(x)} dx \tag{A.12}$$

Using the boundary condition $d(0) = d_0$ the solution of (A.12) is:

$$\begin{aligned} 0 = &\int_{d_0}^{d(x)} Q_1(0,t)\, dt + \int_0^x P_1(t, d(x))\, dt = \\ &\frac{S}{K\, d_0}(B\, d_0^3 + K)^{\frac{1}{3}} - \frac{S + K\, x}{K\, d(x)}(B\, d(x)^3 + K)^{\frac{1}{3}} + \int_{d_0}^{d(x)} \frac{t\, dt}{(B\, t^3 + K)^{\frac{2}{3}}} \end{aligned} \tag{A.13}$$

The solution of the integral in (A.13) is a hyper geometric series. Eq. (A.13) can only be solved numerically. But for the function (A.13) the envelopes can be determined. The first envelope is:

1. $F_w = 0$

Using L'HOSPITAL's rule the first part of Eq. (A.13) becomes:

$$\lim_{K \to 0} \frac{S}{3\, d_0\, (B\, d_0^3 + K)^{\frac{2}{3}}} = \frac{S}{3\, B^{\frac{2}{3}}\, d_0^3}$$

Using L'HOSPITAL's rule the second part of eq. (A.13) becomes:

$$\lim_{K \to 0} \frac{S + K\,x + 3\,x\,(B\,d(x)^3 + K)}{3\,d(x)\,(B\,d(x)^3 + K)^{\frac{2}{3}}} = \frac{S + 3\,x\,B\,d(x)^3}{3\,B^{\frac{2}{3}}\,d(x)^3}$$

and for the integral one gets:

$$\int_{d_0}^{d(x)} \frac{dt}{B^{\frac{2}{3}}\,t} = B^{-\frac{2}{3}}\,\ln\frac{d(x)}{d_0}$$

Assembled and rewritten:

$$0 = \frac{S\,[d(x)^3 - d_0^3]}{3\,d(x)^3\,d_0^3} - B\,z + \ln\frac{d(x)}{d_0} \tag{A.14}$$

The second envelope of (A.13) for ignoring the body weight ($\gamma = 0$) is:

$$\frac{S}{d_0} - \frac{N + K\,z}{d(x)} + \frac{d(x)^2 - d_0^2}{2} = 0$$

Or in normal form:

$$d(x)^3 + \frac{2\,S - d_0^3}{d_0} d(x) - 2\,(S + K\,x) = 0 \tag{A.15}$$

If one ignores the wind load ($F_w = 0$) in eq. (A.7) this equation becomes:

$$\left[d(x)^3 * S + L\,\frac{x^2}{2}\right] d'(x) - d(x)\,[B\,d(x)^3 + L\,x] = 0 \tag{A.16}$$

No integrative factor for (A.16) has been found. The envelopes of (A.16) can be determined. For the first envelope ($q_0 = 0$) the solution of (A.16) is (A.14). For the other envelope ($\gamma = 0$) (A.16) becomes:

$$\left[d(x)^3 + S + L\,\frac{x^2}{2}\right]\,dd(x) - L\,x\,d(x) = 0 \tag{A.17}$$

with

$$P(x,d) = -L\,x\,d(x), \qquad Q(x,d) = d(x)^3 + S + L\,\frac{x^2}{2}$$

because

$$\frac{\partial P}{\partial d} = -L\,x \neq L\,x = \frac{\partial Q}{\partial x}$$

an integrative factor has to be found. Since $\frac{1}{P}\left(\frac{\partial P}{\partial d} - \frac{\partial Q}{\partial x}\right) = \frac{2}{d(x)}$ is only a function of $d(x)$, the integrative factor can be gained as for eq. (A.7). So:

$$\mu = e^{-\int \frac{2}{d} dd} = \frac{1}{d^2}$$

The differential equation (A.17) now reads:

$$0 = \frac{1}{d(x)^2}\left[d(x)^3 + S + L\,\frac{x^2}{2}\right]\,dd(x) - \frac{L\,x}{d(x)}\,dx \tag{A.18}$$

Eq. (A.18) can be integrated:

$$0 = -\frac{L}{d}\int_0^x t\,dt + \int_{d_0}^{d(x)} \frac{1}{t^2}\,(t^3 + S)\,dt$$

or solved:

$$d(x)^3 + \frac{S - d_0^3}{d_0}\,d(x) + \frac{L\,x^2 - 2\,S}{2} = 0 \tag{A.19}$$

B Appendix Least Square

For estimating the model parameters of (10) a Least Square Fit is used. The fit is done with the transformed equation (10) by natural logarithm. For the Least Square Fit one gets:

$$\Theta = \sum_{i=1}^{n}\left\{\ln[d_0] + \frac{\gamma\,\pi\,d_0^2\,x_i}{8\,F_k} - \ln[d(x_i)]\right\}^2 \stackrel{!}{=} \min \tag{B.1}$$

With d_0 the initial diameter of the stem, $\gamma = \rho\, g$ body weight, F_k crown load. $d(x_i)$ and x_i are the data for diameter and height.

A necessary condition for the minimum of the function is that the derivatives of Θ for the parameters F_k and d_0 vanishes:

$$\begin{aligned} 0 = \frac{\partial \Theta}{\partial F_k} &= 2 \sum_{i=1}^{n} \left\{ \ln[d_0] + \frac{\gamma\, \pi\, d_0^2\, x_i}{8\, F_k} - \ln[d(x_i)] \right\} \left(-\frac{\gamma\, \pi\, d_0^2\, x_i}{8\, F_k} \right) \\ 0 = \frac{\partial \Theta}{\partial d_0} &= 2 \sum_{i=1}^{n} \left\{ \ln[d_0] + \frac{\gamma\, \pi\, d_0^2\, x_i}{8\, F_k} - \ln[d(x_i)] \right\} \left(\frac{1}{d_0} + \frac{\gamma\, \pi\, d_0^2\, x_i}{4\, F_k} \right) \end{aligned} \tag{B.2}$$

Resolving the first equation of (B.2) for F_k:

$$F_k = \frac{\gamma\, \pi\, d_0^2 \sum x_i}{8\, [\sum x_i \ln d(x_i) - \ln d_0\ \sum x_i]} \tag{B.3}$$

Inserting (B.3) into the second equation of (B.2) and resolve it for d_0:

$$\ln d_0 = \frac{\sum \ln d(x_i)\ \sum x_i^2 - \sum x_i\ \sum x_i \ln d(x_i)}{n\ \sum x_i^2 - (\sum x_i)^2} \tag{B.4}$$

Resulting in two equations to determine the parameters d_0 and F_k.

References

BENDEROTH, G., SILBER, G., KOLOUPAEV, V., 2000. Mechanical boundary conditions for the growth of plant stems. In: PRENDERGAST, P. J., LEE, T. C., CARR, A. J. (Eds.), Proceedings of the 12th Conference of the European Society of Biomechanics. Dublin: Royal Academy of Medicine in Ireland, p. 415.

BRONSTEIN, I. N. SEMENDJAJEW, A., 1980. Taschenbuch der Mathematik. Harry Deutsch, Thun.

MATTHECK, C., 1990. Engineering components grow like trees. Materialwissenschaft und Werkstofftechnik 21 (143-168).

MATTHECK, C., 1992. Design in der Natur. Rombach, Freiburg.

MATTHECK, C., BETHGE, K., ALBRECHT, W., 1995. Failure modes of trees and related failure criteria. In: COUTTS, M. P. GRACE, J. (Ed.), Wind and Trees. Cambridge University Press, Cambridge.

PETERSON, C. J., 2000. Catasstrophic wind damage to north american forests and the potential impact of climate change. The Science of the Total Environment 265, 287–311.

SILAS, A., 2002. Drag reduction through self-similar bending of a flexible body. Nature 420, 479.

WOOD, C. J., 1995. Understanding wind force on trees. In: COUTTS, M. P. GRACE, J. (Ed.), Wind and Trees. Cambridge University Press, Cambridge.